CHAPTER 4

SINGLE LAYERED CABLE UNDER FREE BENDING - DEVELOPMENT OF NEW MATHEMATICAL MODEL AND VALIDATION

4.1 INTRODUCTION

In an axially loaded single layered stranded cable, each wire undergoes some bending along with axial stretch, as its centerline helix angle varies under load. In general, under axial loading, the conditions of stress and strain of the strand as a whole are assumed to be uniform along the strand axis. However, in bending of strand assembly, such conditions do not hold good except in uniform bending, where the radius of curvature remains constant over a sufficiently long domain. Indeed, uniform curvature bending can be obtained only with surface loads, such as those between a pulley and a strand. Strand behaviour, under such surface loads, is very difficult to analyse. However, in long cables, such assumption of uniform radius of curvature can be maintained only at free field locations, far away from the ends, provided the curvature varies slowly along the strand axis (for example, it should be almost constant over one lay length).

For developing the new thin rod model, a simple strand with a core wire and one layer of six wires with a core-wire type contact, was chosen for comparison. The present model predicts the pre-slip response of the strand under a tensile pre-load and pure and constant curvature free bending in the

absence of an external agency like a sheave employed to enable comparison with available models.

4.2 DEVELOPMENT OF THE GENERAL MATHEMATICAL MODEL

This chapter introduces the formulation of a developed mathematical model to represent a single layered cable assembly to predict the strand axial force, the respective moments of the strand, the effective rigidity, and the contact stresses under free bending condition.

4.2.1 Assumptions and Method of Approach

The effect of wire deformation on the wire curvatures and twist due to strand bending has been considered. The appropriate kinematic variables were derived using Serret-Frenet equations, in order to obtain the constitutive equations. The appropriate expressions for wire forces N and N' were derived by equilibrium methods. The contacts were assumed to be in unlimited coulomb friction. The values of deformation, wire curvatures and torsion were considered for this scenario. The end conditions of the strand are classified into two categories: fixed end and free end conditions. The present mathematical model considered the fixed end conditions. The linear elastic model with wire stretch effect, based on Wempner's (1973) relation has been considered in this work. The new discrete thin rod model was developed with the following assumptions. The core has been assumed to be radially rigid and the Poisson's effects of the core and wires have not been considered.

4.2.2 Stiffness of the Stranded Cable

The Stranded cable global stiffness is derived using the stiffness matrix, relating to the global strand loads to deformations.

$$\begin{Bmatrix} F_a \\ M_t \\ M_b \end{Bmatrix} = \begin{bmatrix} K_{aa} & K_{at} & K_{ab} \\ K_{ta} & K_{tt} & K_{tb} \\ K_{ba} & K_{bt} & K_{bb} \end{bmatrix} \begin{Bmatrix} \varepsilon \\ \delta\chi/h \\ 1/\rho \end{Bmatrix} \tag{4.1}$$

F_a, M_t and M_b are the strand tensile, torsion and bending loads respectively. Likewise ε, $d\chi/h$ and $1/\rho$ are the strand axial strain, rotation per unit length and curvature respectively. K_{aa}, K_{tt}, K_{bb} are effective strand axial stiffness, strand torsional rigidities and flexural rigidities respectively. K_{at}, K_{ta} are the tension – torsion, K_{ab}, K_{ba} are the tension – bending and K_{tb}, K_{bt} are the torsion – bending coupling parameters respectively.

4.2.3 Wire Curvatures and Twist

For an initially straight strand configuration, the components of wire curvatures and wire twist (without slip) in the normal, bi-normal and axial directions are given as

$$\kappa_0 = 0\,,\ \kappa_0' = \frac{\cos^2\alpha}{r}\,,\ \tau_0 = \frac{\sin\alpha\cos\alpha}{r} \tag{4.2}$$

Let the wires in the strand be deformed under the action of the combined effect of axial load and bending. Then the final curvatures and twist of a helical wire are given by

$$\kappa_1 = \kappa_0 + \Delta\kappa\,,\ \kappa_1' = \kappa_0' + \Delta\kappa'\,,\ \tau_1 = \tau_0 + \Delta\tau \tag{4.3}$$

Ramsey (1988 & 1990) developed the relations for the wire flexural strains about the wire normal and wire binormal axis and the torsional strain about the wire axis. Wempner (1973) derived the general expressions for curvatures and torsion for wire rotation alone first and he then extended the same for wire rotation combined with wire stretch. Based on these theories, Sathikh et al (1996) derived expressions for changes in curvature in normal

and binormal wire axis, and for change in twist about the wire axis. Further, Sathikh et al (2000) derived expressions for pure bending loading conditions as given in Equation (4.1) were all the stiffness coefficients other than K_{bb} are zero.

The present work includes the strong coupling between "axial and bending" and "torsion and bending" loads. This is achieved by deriving the expression for coupling stiffness coefficients namely K_{ab}, K_{ba}, K_{tb} and K_{bt} in Equation 4.1. However the basis of the remaining coupling can be regarded as the assemblage of two models: 1. Axial only (Sathikh et al 1996) and 2. Pure bending only (Sathikh et al 2000). The need for the development of the present model arise in many situations where a strand is subjected to simultaneous axial and bending loading condition such as a sagging of overhead transmission cable etc. The present works distinguishes itself from the other works by satisfying the above need in a consistent way.

The curvatures and twist of a helical wire subjected to a combination of axial deflection and bending of a strand are given by

$$\Delta\kappa = \frac{\sin\alpha\left(1+\cos^2\alpha\right)\sin\phi}{\rho} \tag{4.4}$$

$$\Delta\kappa' = \frac{-\sin^2\alpha\cos^2\alpha}{r}\varepsilon + \sin\alpha\cos\alpha\left(1+\sin^2\alpha\right)\frac{\delta\chi}{h} + \frac{\sin^4\alpha\cos\phi}{\rho} \tag{4.5}$$

$$\Delta\tau = \frac{\sin\alpha\cos^3\alpha}{r}\varepsilon + \sin^4\alpha\frac{\delta\chi}{h} - \frac{\sin^3\alpha\cos\alpha\cos\phi}{\rho} \tag{4.6}$$

4.2.4 Wire Shear Forces *N* and *N'*

As noted by Sathikh et al (2000), ignoring the second order effects

of curvatures and twist, the following expressions for wire shear forces N and N' of helical wire subjected to a combination of axial deflection and bending were derived in cognizance with Wempner's (1973) approach.

$$N = -G\tau_0 = \frac{-G\sin\alpha\cos\alpha}{r} \tag{4.7}$$

$$N' = H\kappa_0' - G'\tau_0 = \frac{(H\cos\alpha - G'\sin\alpha)\cos\alpha}{r} \tag{4.8}$$

4.2.5 Constitutive Equations

In the present case of constant strand curvature free bending, a uniform external bending moment is assumed. G, G' are the components of the wire bending moment on a wire cross section in the normal and bi-normal direction respectively. T and H are the axial tension and twisting moment in the axial direction of the wire. These wire components are shown in Figure 3.2. The constitutive equations are given by

$$T = EA\sin^2\alpha\,\varepsilon + EAr\sin\alpha\cos\alpha\frac{\delta\chi}{h} + \frac{EAr\sin^2\alpha\cos\phi}{\rho} \tag{4.9}$$

$$G = \frac{EI\sin\alpha(1+\cos^2\alpha)\sin\phi}{\rho} \tag{4.10}$$

$$G' = \frac{-EI\sin^2\alpha\cos^2\alpha}{r}\varepsilon + EI\sin\alpha\cos\alpha(1+\sin^2\alpha)\frac{\delta\chi}{h} + \frac{EI\sin^4\alpha\cos\phi}{\rho} \tag{4.11}$$

$$H = \frac{CJ\sin\alpha\cos^3\alpha}{r}\varepsilon + CJ\sin^4\alpha\frac{\delta\chi}{h} - \frac{CJ\sin^3\alpha\cos\alpha\cos\phi}{\rho} \tag{4.12}$$

$$N = -\frac{EI\sin^2\alpha\cos\alpha\left(1+\cos^2\alpha\right)\sin\phi}{r\rho} \tag{4.13}$$

$$\begin{aligned} N_i' = &\left(\frac{CJ\sin\alpha\cos^5\alpha}{r^2} + \frac{EI\sin^3\alpha\cos^3\alpha}{r^2}\right)\varepsilon \\ &+\left(\frac{CJ\sin^4\alpha\cos^2\alpha}{r} - \frac{EI\sin^2\alpha\cos^2\alpha\left(1+\sin^2\alpha\right)}{r}\right)\frac{\delta\chi}{h} \\ &+\left(-\frac{CJ\sin^3\alpha\cos^3\alpha\cos\phi}{r} - \frac{EI\sin^5\alpha\cos\alpha\cos\phi}{r}\right)\frac{1}{\rho} \end{aligned} \tag{4.14}$$

4.2.6 Equilibrium Equations of Stranded Cable

The resultant external axial force, twisting moment and bending moment of the stranded cable have the wire components from Equations (4.9) to (4.14). All the forces on the core and the wires are projected along the axial direction of the strand and this is given by Equation (4.15)

$$F_a = \left(m\left[T\sin\alpha + N'\cos\alpha\right]\right) + E_c A_c \varepsilon \tag{4.15}$$

The total axial twisting moment acting on the central wire and the surrounding wires are given by Equation (4.16)

$$M_t = \left(m\left[H\sin\alpha + G'\cos\alpha + Tr\cos\alpha - N'r\sin\alpha\right]\right) + C_c J_c \frac{\delta\chi}{h} \tag{4.16}$$

The bending moment of the central wire and the surrounding wires are given by the Equation (4.17)

$$M_b = \left(m\left[\begin{array}{l}\left(T\sin\alpha + N'\cos\alpha\right)r\cos\phi - H\cos\alpha\cos\phi \\ +G\sin\phi + G'\sin\alpha\cos\phi - Nr\dfrac{\cos\alpha}{\sin\alpha}\sin\phi\end{array}\right]\right) + \frac{E_c I_c}{\rho} \tag{4.17}$$

The stiffness coefficients for coupling parameters of all the wires in a layer and the core are given by the Equations (4.18) to (4.26).

$$K_{aa} = E_c A_c + m\left(EA\sin^3\alpha + \frac{GJ\sin\alpha\cos^6\alpha}{r^2} + \frac{EI\sin^3\alpha\cos^4\alpha}{r^2} \right) \tag{4.18}$$

$$K_{at} = m\begin{pmatrix} EAr\sin^2\alpha\cos\alpha + \dfrac{GJ\sin^4\alpha\cos^3\alpha}{r} \\ -\dfrac{EI\sin^2\alpha\cos^3\alpha\left(1+\sin^2\alpha\right)}{r} \end{pmatrix} \tag{4.19}$$

$$K_{ab} = m\begin{pmatrix} EAr\sin^3\alpha\cos\phi - \dfrac{GJ\sin^3\alpha\cos^4\alpha\cos\phi}{r} \\ -\dfrac{EI\sin^5\alpha\cos^2\alpha\cos\phi}{r} \end{pmatrix} \tag{4.20}$$

$$K_{ta} = m\begin{pmatrix} \dfrac{GJ\sin^2\alpha\cos^3\alpha}{r} - \dfrac{EI\sin^2\alpha\cos^3\alpha}{r} + EAr\sin^2\alpha\cos\alpha \\ -\dfrac{GJ\sin^2\alpha\cos^5\alpha}{r} - \dfrac{EI\sin^4\alpha\cos^3\alpha}{r} \end{pmatrix} \tag{4.21}$$

$$K_{tt} = G_c J_c + m\begin{pmatrix} GJ\sin^5\alpha + EI\sin\alpha\cos^2\alpha\left(1+\sin^2\alpha\right) \\ +EAr^2\sin\alpha\cos^2\alpha - GJ\sin^5\alpha\cos^2\alpha \\ +EI\sin^3\alpha\cos^2\alpha\left(1+\sin^2\alpha\right) \end{pmatrix} \tag{4.22}$$

$$K_{tb} = m\begin{pmatrix} -GJ\sin^4\alpha\cos\alpha\cos\phi + EI\sin^4\alpha\cos\alpha\cos\phi \\ +EAr^2\sin^2\alpha\cos\alpha\cos\phi \\ +GJ\sin^4\alpha\cos^3\alpha\cos\phi + EI\sin^6\alpha\cos\alpha\cos\phi \end{pmatrix} \tag{4.23}$$

$$K_{ba} = m\begin{pmatrix} EAr\sin^3\alpha\cos\phi + \dfrac{GJ\sin\alpha\cos^6\alpha\cos\phi}{r} \\ +\dfrac{EI\sin^3\alpha\cos^4\alpha\cos\phi}{r} \\ -\dfrac{EI\sin^3\alpha\cos^2\alpha\cos\phi}{r} - \dfrac{GJ\sin\alpha\cos^4\alpha\cos\phi}{r} \end{pmatrix} \tag{4.24}$$

$$K_{bt} = m\begin{pmatrix} EAr^2 \sin^2\alpha\cos\alpha\cos\phi + GJ\sin^4\alpha\cos^3\alpha\cos\phi \\ -EI\sin^2\alpha\cos^3\alpha\left(1+\sin^2\alpha\right)\cos\phi \\ +EI\sin^2\alpha\cos\alpha\left(1+\sin^2\alpha\right)\cos\phi \\ -GJ\sin^4\alpha\cos\alpha\cos\phi \end{pmatrix} \quad (4.25)$$

$$K_{bb} = E_c I_c + m\begin{pmatrix} EAr^2\sin^3\alpha\cos^2\phi - GJ\sin^3\alpha\cos^4\alpha\cos^2\phi \\ -EI\sin^5\alpha\cos^2\alpha\cos^2\phi + EI\sin^5\alpha\cos^2\phi \\ +GJ\sin^3\alpha\cos^2\alpha\cos^2\phi \\ +EI\sin\alpha\cos^2\alpha\left(1+\cos^2\alpha\right)\sin^2\phi \\ +EI\sin\alpha\left(1+\cos^2\alpha\right)\sin^2\phi \end{pmatrix} \quad (4.26)$$

4.3 DEVELOPMENT OF THE FINITE ELEMENT MODEL

The finite element model for the single layered cable was developed such that the core was extruded along the strand axis while each wire in the layer was extruded of its cross-section, along a helix (multi linear curve). The model was developed for two pitch lengths. The commercial Finite Element Analysis software "ANSYS" has been used. Three dimensional solid brick elements have been used for structural discretization. Each node has three degrees of freedom, i.e. translation x, y and z directions. Contact between the core and the wire has been modeled using surface contact elements.

An available 'Master – Slave node concept' was used to define the rigid regions at both the ends of the strand. Multiple constraint equations to relate nodal degrees of the freedom in defined region are generated by this concept. The nodes at the loading ends of both sides of the strand were separately grouped to act as 'slave nodes'. An additional node called master node, which is the retained node for the rigid region was created on the axis of the core at a distance away from both ends of the slave nodes. This master

node facilitates the loading and extraction of reaction forces and moments. By means of constraint equations, the slave nodes at either ends of the strand were linked using rigid body elements to the master node to have the same displacement as defined by the master node. The boundary conditions required to simulate free bending has been achieved as mentioned below.

The master nodes at the either ends of the strand were fully clamped by constraining all degrees of freedom (d.o.f) of the nodes except for rotation about x axis. Then, the symmetric bending rotations about x axis ranging from 0 to 0.01 radians were enforced at the end points as shown in Figure 4.1.

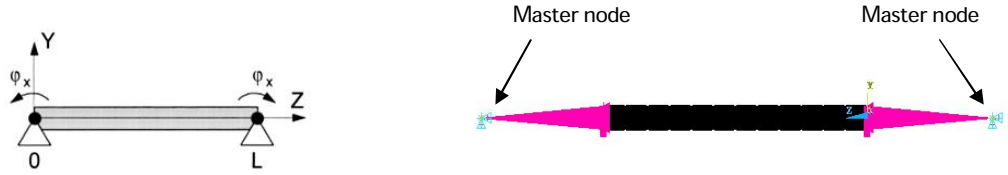

(a) Free body diagram **(b) FE model of undeformed strand**

Figure 4.1 Free bending of the strand

4.3.1 Parameters of the Cable

The geometrical data has been adopted from LeClair and Costello (1988) to study the bending response. The numerical data of the strand considered is presented in Table 4.1.

Table 4.1 Numerical data for single layered stranded cable

Parameter	Symbol	Values
Number of helical wires	m	6
Radius of core	R_c	0.787 mm
Radius of helical wire	R_w	0.737 mm
Helix angle	α	70°
Young's modulus for core and wire	E_c & E_w	207×10^3 N/mm^2
Poisson's ratio	υ	0.3
Position angle of helical wires strand	ϕ	0° to 360°

4.4 RESULTS AND DISCUSSION

In the present investigation, the common response parameter for comparison between analytical and FEA models was identified as the resulting bending moment. However the input for FEA model is in terms of rotation while for the analytical model it is the curvature of strand axis. Rotations about x axis ranging from 0 to 0.01 radians in four steps were enforced at the master nodes of the FEA model to simulate symmetric bending load. The resulting radii of curvature for respective steps of rotations were obtained by tracing the deformed curve of the strand axis. And, the strand bending moments for each step of rotation were determined at the master nodes. Then the radii of curvature of the strand axis obtained from FEA model was supplied as input to the analytical model and the bending moments were thus computed. The resulting bending moments from both the models for various curvatures of strand axis have been plotted in the Figure 4.2.

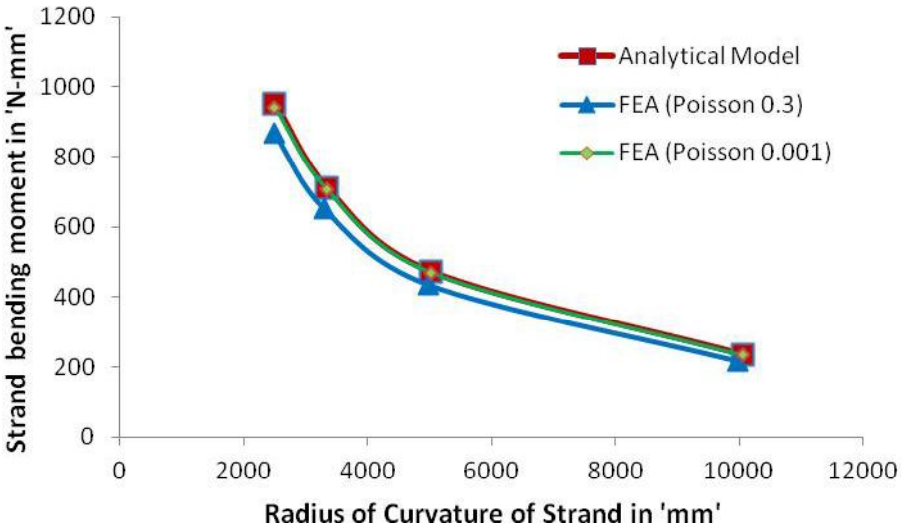

Figure 4.2 Variation of bending moment as a function of radius of curvature

It is seen from Figure 4.2 that the present analytical model agrees well with the results of FE analysis. In the analytical model, as addressed earlier the core and wires were assumed to be radially rigid. Here the value of Poisson's ratio for the core and wires were assumed to be very low with a value of 0.001 in the FE analysis. A separate FE analysis was rerun with a Poisson's ratio of 0.3, to study its effects on the response. The Figure 4.2 also shows the variation in response of the strand bending moment for different values of Poisson's ratio. It could be observed that for the same range of variation of curvatures, the FE analysis with Poisson's value of 0.3 differs from that of the values with poisson's ratio of 0.001 by 8.5%.

In most of the published literature to date, only analytical models have been applied to simple bending cases. The influence of more complicated factors such as stresses due to bending moment, contact stress etc on the behavior of strand is very difficult if not possible to predict analytically. It is noted that such parameters have strong influence on the

mechanism of cable failure. Therefore, there is a requirement for a general and more accurate FE model (strand) which is capable of taking into account the complicating factors such as contact stress. With the development of the finite element method, it is now possible to analyse more complex behavior. The Figure 4.3 shows the undeformed and deformed configurations of the strand for 0.01 radians of rotation of the master node.

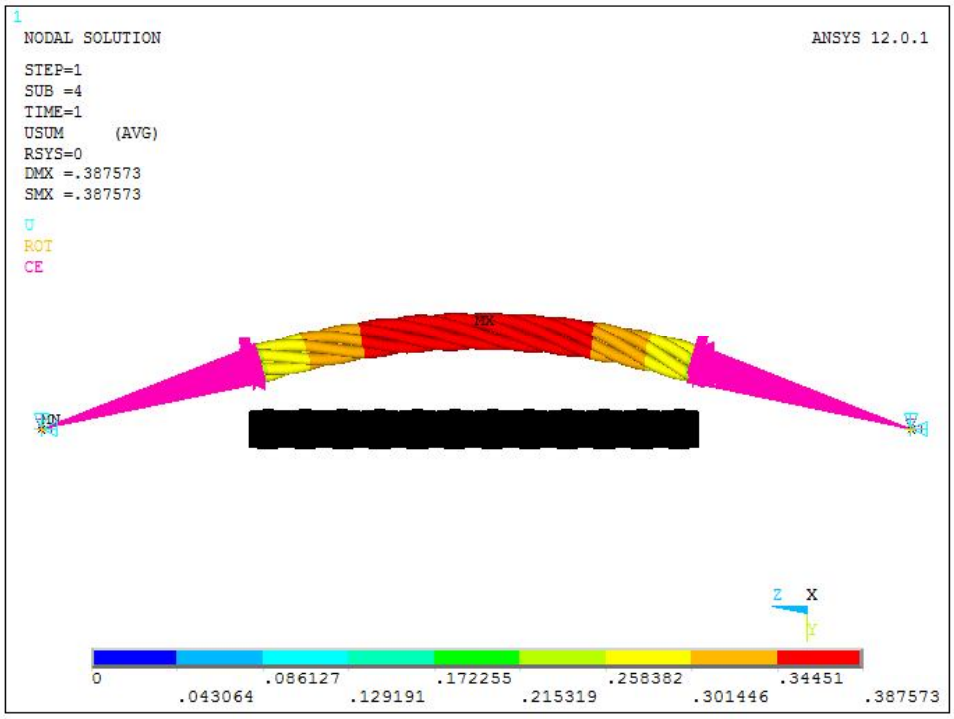

Figure 4.3 Deformed and undeformed configuration of the cable

It may be noted that the wires in the outer layer make a continuous ‘helical line contact’ with the core. The contact lines showing the helical line contact and the contact stress determined through the FE analysis for the strand for 0.01 radians of rotation of the master node is shown in Figure 4.4.

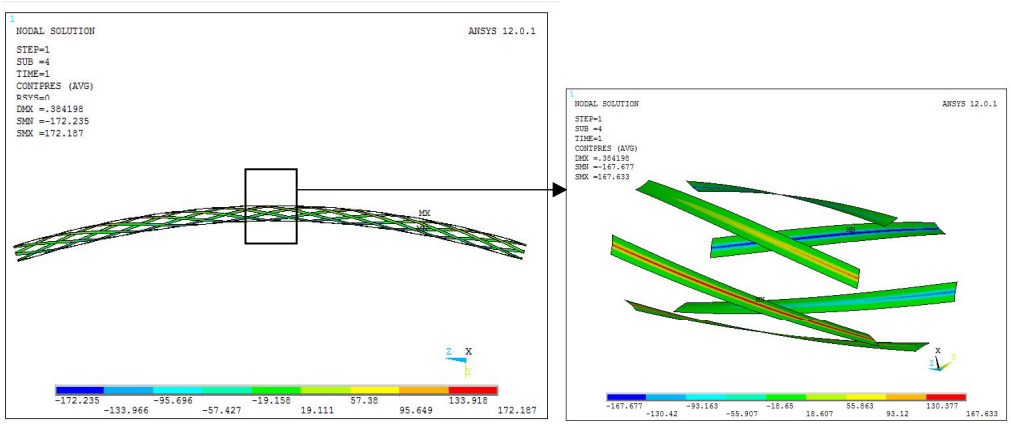

Figure 4.4 Contact pressure at the helical line contact at the mid span of the cable

The dependence of the maximum contact pressure against the various curvatures is shown in Figure 4.4. It is worth to mention that the numerical analyses performed were based on idealised perfect geometric strand model (for verification purpose with the analytical model), such that there was no relative motion between the core and the wires. Hence such high values of contact pressure were reported. In reality, a relative movement takes place between all contact surfaces due to the tendency of the helical angle to change when the load changes. The magnitude of relative movements depends on the magnitude of the applied bending curvature and angular location of the contact points relative to the bending direction. In such cases the contact pressure along the contact lines was observed to be relatively small for the range curvatures mentioned above.

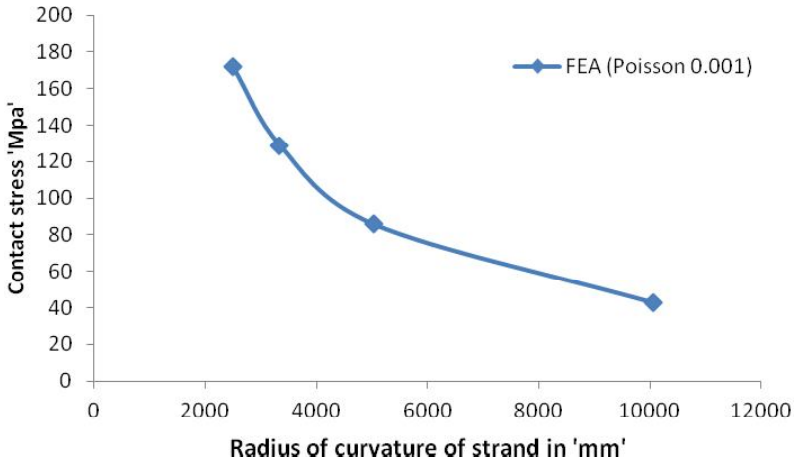

Figure 4.5 Dependence of maximum contact stress on various radius of curvature of the strand

Since the model is based on linear theory, a linear increase of the contact pressure is observed for the range of radius of curvatures mentioned in Figure 4.5.

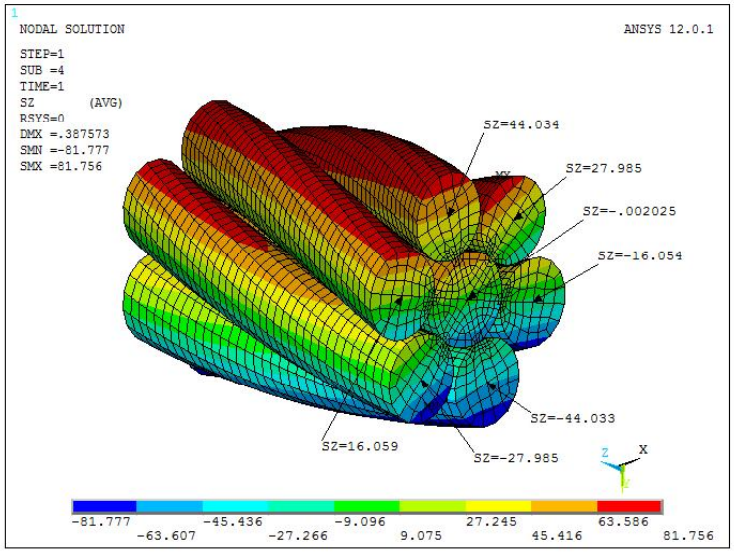

Figure 4.6 Distribution of bending stress over the cross section of the cable at its mid span

Figure 4.6 presents a sample bending stress distribution on the strand cross-section with a radius of curvature of the strand as 2.5 m, which is a typical worst case loading level in engineering applications of overhead electrical transmissions.

The Figure 4.7 shows the typical wire bending stress pattern over all the wire cross-sections. The wires on the top as expected are subjected to tensile stress and the bottom wires are subjected to compressive stresses. The distribution of stress over a cross section of the strand which is very difficult if not possible to predict analytically, can now be determined using FE analysis.

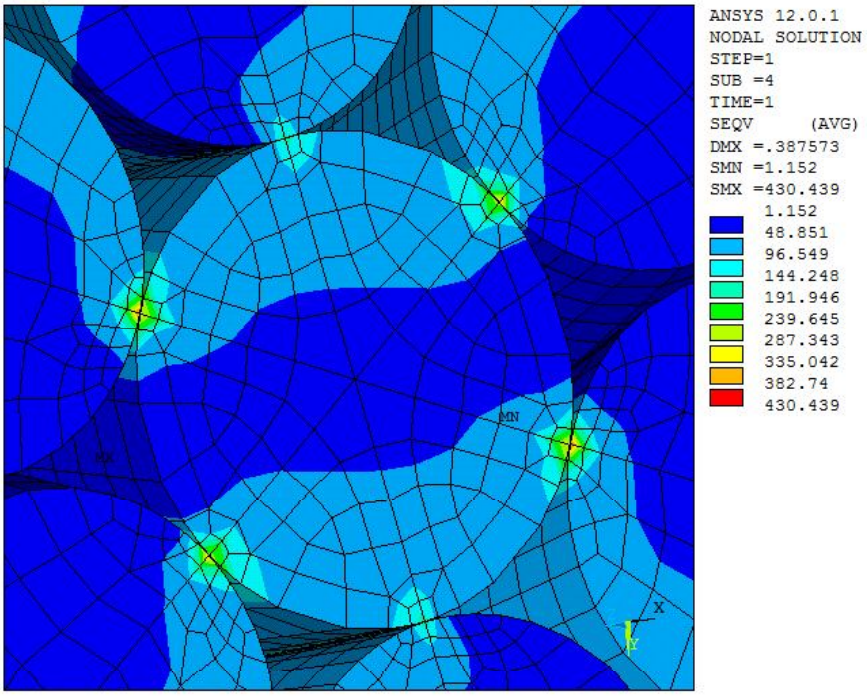

Figure 4.7 von Mises stress distribution recorded at the mid span of the cable length

It is seen from the legend that the peak stresses are located very close to the contact surfaces and that the highest stress are at the contact

junctions corresponds to the contact between the core and the helical wires. There is thus, scope for further studies to look into the contact mechanics of cable assemblies under bending.

4.5 CONCLUSION

A model was developed to describe the bending behaviour of the single layer stranded cable. The present work distinguishes itself from the earlier works of other authors by accommodating the strong coupling terms namely the “axial–bending” and “torsion-bending”. This improved analytical expression was examined on the prevailing geometry to predict the bending moment of the cable.

Finite element model for the single layered cable assembly was also developed for the free bending of the cable. A simulation was conducted and the variation of bending moment for various applied radii of curvature and stress intensities across the cross-section was determined. The findings have been reported in the section 4.4.